



Cite this: *RSC Adv.*, 2017, 7, 28207

pH-responsive magnetic micelles gelatin-*g*-poly(NIPAAm-*co*-DMAAm-*co*-UA)-*g*-dextran/Fe₃O₄ as a hydrophilic drug carrier†

Chao-Ming Su,^a Chen-Yu Huang,^b Yao-Li Chen^c and Tzong-Rong Ger^{*a}

pH-responsive magnetic micelles are beneficial for time-controlled and site-specific drug delivery without triggering potential biological side effects. In this study, gelatin-*g*-poly(NIPAAm-*co*-DMAAm-*co*-UA)-*g*-dextran/Fe₃O₄ (GPDF) pH-responsive magnetic micelles were synthesized to carry a hydrophilic insulin-promoting factor, nicotinamide. The chemical structures were analyzed *via* Fourier transform infrared spectroscopy (FTIR) and nuclear magnetic resonance (NMR) spectroscopy. Superconducting quantum interference device (SQUID) analysis confirmed the superparamagnetic property of the GPDF micelle. The accumulative nicotinamide release under pathological pH conditions (pH 6.6) was found to be three-fold higher than that under normal pH conditions (pH 7.2). The results suggest that GPDF is beneficial for a pH-selective and magnetic target-controlled release drug delivery system.

Received 8th February 2017
 Accepted 29th April 2017

DOI: 10.1039/c7ra01633f

rsc.li/rsc-advances

Introduction

Polymeric micelles composed of copolymers can self-assemble to form a core/shell structure through hydrophobic/hydrophilic interaction in aqueous solutions. Their hydrophilic shell not only stabilizes the micelles but also helps them escape clearance by the reticuloendothelial system (RES), which greatly increases blood half-life and treatment efficiency.^{1,2} Moreover, the unique hydrophobic/hydrophilic portions of polymeric micelles allow them to carry drugs of different polarity.³ Until recently, polymeric micelles have been used as carriers for cancer therapy,^{4–7} protein,^{8,9} and imaging agents.^{10–12} For more advanced approaches, stimuli-responsive polymeric micelles that promote drug release *via* the variation of environmental factors, such as light,^{13,14} pH,¹⁵ redox potential,^{16,17} or/and temperature,^{18,19} or multi-factors,²⁰ have been investigated for their drug loading capacity and delivery efficiency.

Moreover, several temperature-responsive polymers, such as poly(*N*-isopropylacrylamide) (poly(NIPAAm)),^{21,22} poly(*N*-vinylcaprolactam) (PNVCL),²³ and poly(2-alkyl/aryl-2-oxazoline)s (PAOx),²⁴ have been reported for controlled drug delivery. Specifically, poly(NIPAAm) is the most commonly used polymer with a lower critical solution temperature (LCST) at about 32 °C in aqueous media. When the temperature is above the LCST, poly(NIPAAm) become hydrophobic because of the temporary

breakage of the hydrogen bonds. Under the pathology conditions caused by inflammation or cancer, the extracellular pH value has been found to be lower than that under normal conditions.²² By introducing hydrophilic or hydrophobic segments (*e.g.*, poly(10-undecenoic acid)) with pH sensitive features, the LCST of poly(NIPAAm) at different pH environments can be varied; therefore, it can also be transformed into pH-responsive micelles for selective drug delivery.^{25,26}

To increase poly(NIPAAm) micelles' biocompatibility, bioactivity and biodegradability, natural polymers such as aspartic acid,^{27,28} gelatin,^{29–31} and chitosan^{32,33} can be incorporated. In particular, gelatin has high water absorption characteristics, which are beneficial for micelles to load hydrophilic molecules.³⁴

Magnetic nanoparticles (MNPs) are chemically stable, nontoxic, cost-efficient, and suitable for a variety of biomedical applications.^{35,36} Through incorporating MNPs with pH-responsive micelles, drugs can be delivered to selective regions or for magnetic targeting and magnetic resonance imaging (MRI) applications. To incorporate MNPs, researchers have tried different strategies, either by conjugating MNPs on the surface of the micelle³⁷ or encapsulating MNPs inside the micelle.³⁸

In this study, we synthesized copolymer gelatin-*g*-poly(NIPAAm-*co*-DMAAm-*co*-UA)-*g*-dextran/Fe₃O₄ pH-responsive magnetic micelles for pH and magnetic targeting treatment. *N,N*-Dimethyl acrylamide (DMAAm) was used to adjust the LCST of the micelles, and gelatin improved the biocompatibility and regulated the LCST. Poly(10-undecenoic acid) was used to introduce pH-sensitive fragments. Dextran/Fe₃O₄ MNPs were grafted on the surface of the pH-responsive micelles for magnetic targeting. Hydrophilic insulin-promoting factor, nicotinamide, was used for the study of controlled release drug delivery.

^aDepartment of Biomedical Engineering, Chung Yuan Christian University, Taoyuan, Taiwan. E-mail: sunbow@cycu.org.tw

^bDepartment of Physics and Astronomy, Johns Hopkins University, Baltimore, MD, USA

^cDepartment of General Surgery, Changhua Christian Hospital, Changhua, Taiwan

† Electronic supplementary information (ESI) available. See DOI: 10.1039/c7ra01633f



Materials and methods

Materials

Sodium dodecyl sulfate, CM-dextran, *N,N*-dimethyl acrylamide (DMAAm), *N*-isopropylacrylamide (NIPAM), sodium hydroxide (NaOH), methyl-3-mercaptopropionate (MMP), sodium dodecyl sulfate (SDS), 1-ethyl-3-(3-dimethylaminopropyl)carbodiimide hydrochloride (EDC), *N*-hydroxysuccinimide (NHS), 1,6-diphenyl-1,3,5-hexatriene (DPH), ferrous chloride hexahydrate ($\text{FeCl}_2 \cdot 6\text{H}_2\text{O}$), and nicotinamide were purchased from Sigma Aldrich (MO, USA). Dialysis membrane (1000 or 50 000 MWCO) was obtained from Spectrum Laboratories, Inc. (CA, USA). 10-Undecenoic acid (UA) and hydrazine were purchased from Alfa Aesar (MA, USA). Potassium persulfate, methanol, potassium bromide (KBr), and ferrous chloride tetrahydrate ($\text{FeCl}_2 \cdot 4\text{H}_2\text{O}$) were received from J. T. Baker (NJ, USA). All chemicals, reagents, and solvents were used without further purification.

Synthesis of CM-dextran/ Fe_3O_4

CM-dextran/ Fe_3O_4 was prepared *via* a co-precipitation method according to a previous study.²⁸ A three-necked flask was degassed with nitrogen for 30 min. Then, 30 mL deionized water was injected into the flask and heated to 80 °C. FeCl_3 and CM-dextran were dissolved in 10 mL deionized water and injected into the flask. After 5 min, 0.835 mL of hydrazine was added to the solution to reduce the particle size and increase particle saturation magnetization. A mixture of FeCl_2 and deionized water was then injected into the flask after another 5 min. After completely mixing the solution, eight mL of 1 N sodium hydroxide was slowly added to the mixture. The solution was dialyzed (MWCO > 50 000 Da) and freeze-dried to obtain CM-dextran/ Fe_3O_4 .

Synthesis of poly(NIPAAm-*co*-DMAAm-*co*-UA)

The process of synthesis of poly(NIPAAm-*co*-DMAAm-*co*-UA) is described in Fig. 1a. Herein, 9 mmol of NIPAAm, 1 mmol of DMAAm, and 0.2 g SDS were dissolved in 10 mL deionized water under stirring at 300 rpm. Then, 1 mmol UA in 5 mL deionized water was added, and the pH value of the solution was adjusted to 6.7 by 1 N NaOH. The solution was then degassed by nitrogen for 30 min and heated to 70 °C. MMP and potassium persulfate (KPS) were dissolved in 10 mL deionized water and added into the mixture and reacted at 70 °C for 4 h. The solution was then dialyzed for 4 to 6 h using a dialysis membrane (MWCO > 1000 Da). Finally, the polymer poly(NIPAAm-*co*-DMAAm-*co*-UA) CO_2CH_3 (PNDU) was obtained after freeze-drying (Fig. 1a).

Herein, 0.2 g of PNDU was mixed in 50 mL methanol with 36 μL hydrazine. The mixture was refluxed at 90 °C for 3 h and dialyzed (MWCO > 1000 Da) for 9 h. Poly(NIPAAm-*co*-DMAAm-*co*-UA)-CONHNH₂ (PNDU-NH₂) was obtained after freeze-drying (Fig. 1b).

Synthesis of gelatin-*g*-poly(NIPAAm-*co*-DMAAm-*co*-UA)

Gelatin was then grafted on PNDU-NH₂ *via* EDC/NHS reaction by radical copolymerization, as described in a previous study.

Herein, 60 mg gelatin was dissolved in a 3 mL of EDC/NHS solution (200 mM of EDC and 50 mM of NHS in deionized water) and incubated for 90 min to activate the carboxyl group of gelatin. Then, 60 mg of PNDU-NH₂ was added into EDC/NHS-activated gelatin solution and the reaction was allowed to proceed at 25 °C for 85 min. The solution was dialyzed (MWCO > 50 000 Da) against deionized water for 1 day to remove the ungrafted polymers. Finally, gelatin-*g*-poly(NIPAAm-*co*-DMAAm-*co*-UA) (gelatin-*g*-PNDU, GP) was obtained after freeze-drying (Fig. 1c).

Preparation of gelatin-*g*-PNDU-*g*-dextran/ Fe_3O_4

Herein, 10 mg of CM-dextran/ Fe_3O_4 was dissolved in 3 mL EDC/NHS solution for carboxyl group activation. After 90 min, GP was added to the mixture and allowed to react for 85 min. The solution was then dialyzed (MWCO > 1000 Da) for 1 day. Gelatin-*g*-poly(NIPAAm-*co*-DMAAm-*co*-UA)-*g*-dextran/ Fe_3O_4 (gelatin-*g*-PNDU-*g*-dextran/ Fe_3O_4 , GPDF) was obtained after freeze-drying (Fig. 1d).

Characteristic analysis

Fourier transform infrared spectroscopy (FTIR) and nuclear magnetic resonance (NMR) analysis were performed to assess the chemical properties. FTIR was used to determine whether gelatin was grafted on PNDU; three groups of sample: GP, PNDU, and gelatin, were mixed with KBr and pressed into the disc for measurement by an FTIR spectrometer (FT/IR-4200 (Jasco, Japan)). The grafting ratio of the copolymers was then determined using an NMR spectrometer (500 MHz NMR Spectrometer (Bruker, Germany)). The sample was dissolved in DMSO-*d*₆ for the grafting ratio analysis. The particle size of the micelles was measured using dynamic light scattering (DLS) (LS series (Beckman Coulter, USA)). The concentration of the polymer solution was higher than the critical micelle concentrations (CMC), and the solution was filtered by a 0.45 mm filter. A drop of the solution was placed on a copper grid to measure the particle size using a transmission electron microscope (TEM) (JEM-200CX (JEOL, Japan)). Sample dissolved in PBS was analyzed by a UV-vis spectrometer (V-530, Jasco, Japan) to investigate the absorbance at the wavelength of 200–350 nm.

Thermogravimetric analysis

The percentage of dextran/ Fe_3O_4 grafted on GP was identified by thermogravimetric analysis (TGA) (DuPont, USA, TA Q50). Herein, 2 mg of samples were placed on a platinum pan, the analysis was carried out in a nitrogen flow, and the samples were heated to reach 600 °C at a heating rate of 20 °C min.

Phase transition characterizations

The phase transition characteristics of GP or PNDU were measured by a UV-vis spectrophotometer at 500 nm, and the temperature was monitored by a thermometer (T319, Tecpel, Taiwan). GP or PNDU were dissolved in PBS at different pH values. The solution was heated to 55 °C and the temperature was gradually reduced. The transmittance was then measured,



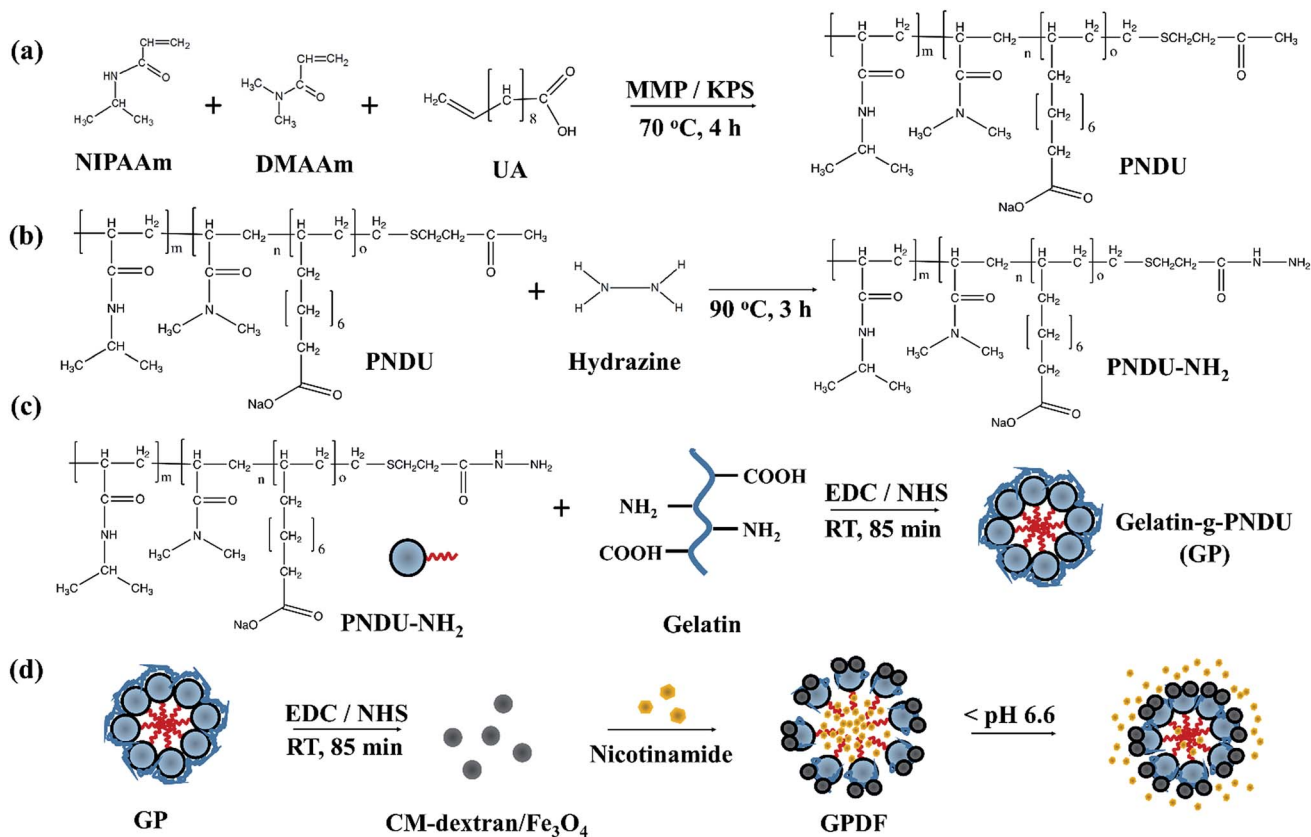


Fig. 1 Schematic of the formation of gelatin-*g*-dextran/Fe₃O₄ (GPDF) (a) synthesis of PNDU, (b) modification of PNDU to PNDU-NH₂, (c) preparation of gelatin-*g*-PNDU (GP) from gelatin and PNDU-NH₂ by EDC/NHS coupling, and (d) formation of GPDF by grafting CM-dextran/Fe₃O₄ to GP via EDC/NHS coupling and then loaded with nicotinamide to test drug release at pH value < 6.6.

corresponding to the decrease in temperature. The phase transition is defined by the temperature at which the transmittance is decreased to half.

Drug load and release studies

To load micelles with insulin-promoting factor, nicotinamide, 10 mg of GPDF was firstly dissolved in 2 mL of deionized and then 10 mg nicotinamide was added into the solution. After this, 6 mL of acetone was added dropwise and incubated for 2 h, the supernatant was siphoned off, and the precipitate was dried at room temperature to obtain the nicotinamide-loaded GPDF micelles. The accumulative nicotinamide release was tested at pH 7.2 and pH 6.6 in PBS at 37.5 °C. The absorbance of nicotinamide was measured at 274 nm by a UV/vis spectrophotometer to investigate the amount of the drug released. The cumulative percent drug release was determined by analyzing the weight of the initial absorbed drug in the micelle and the weight of the released drug in the solution.

Results and discussion

In the study, gelatin was used to adjust the LCST of the pH-responsive micelles. As shown in Fig. 2, PNDU has the symmetrical stretching vibration of -CH₃ and C=O groups at 2972 and 1648 cm⁻¹, respectively. The absorption peaks at 1543

and 1461 cm⁻¹ of PNDU showed the presence of -OH and C=O, respectively. The absorption peaks at 2940 and 1238 cm⁻¹ respectively showed the presence of -CH and amide III groups of gelatin, which confirmed the successful incorporation of gelatin in the GP polymer.

CM-dextran/Fe₃O₄ were then grafted on GP to introduce pH-responsive micelles with the magnetic responsive property. In

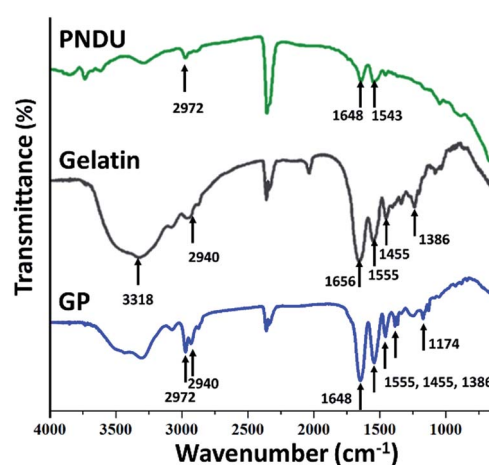


Fig. 2 FT-IR spectra of PNDU, gelatin, and GP.



Fig. 3, GPDF shows the absorption peaks of the C=O group at 1648 cm^{-1} found in GP, the vibration located at 1017 cm^{-1} , attributed to the C–O stretch of dextran, and 570 cm^{-1} of Fe–O, which prove the successful grafting of GP and CM-dextran/ Fe_3O_4 in GPDF.

Structural elucidation and verification of GPDF were carried out using ^1H NMR spectroscopy, as shown in Fig. 4. The characteristic peaks of methyl in NIPAAm of GPDF are shown at 1.04 and 3.85 ppm. The characteristic peaks at 4.47–4.92 ppm correspond to dextran of GPDF. The hydrogen atom of β and γ - CH_2 of arginine appeared at 1.94 ppm. The data confirmed that PNDU was grafted with gelatin *via* an amide reaction. Moreover, the carboxylic group of CM-dextran bound to GP *via* amide bond formation and resulted in the final GPDF product.

From the data shown in Table 1, the LCST of PNDU were 31.4 and $32.3\text{ }^\circ\text{C}$ at pH 6.6 and 7.2, respectively, and it exhibits pH-responsivity. However, to be more beneficial for controlled-release systems that specifically identifies lesions to normal tissue through environmental pH difference, gelatin was grafted on PNDU, resulting in LCST being increased without affecting pH-responsivity of micelles and improving the usage of the micelle for the human body (seen Table 1 GP). Moreover, after modifying GP micelles with CM-dextran/ Fe_3O_4 , no obvious difference in the LCST of GP and GPDF were seen, which could prove that the grafting of CM-dextran/ Fe_3O_4 did not change the balance of hydrophilicity and hydrophobicity of the micelles and gave the micelle a magnetic responsive property.

TEM was used to observe the morphology of GP or GPDF micelles. The TEM image, as shown in Fig. 5a, depicts that GP micelles formed a spheroidal structure with a hydrophilic shell and a hydrophobic core. The GPDF has a zeta potential of $-6.35 \pm 0.28\text{ mV}$ in water and a value close to zero (-0.13 mV) in DMSO, which confirm that GPDF has a negatively-charged shell layer and a neutral core in aqueous solution (in Fig. S2 of ESI†). MNPs attached to the surface of GPDF micelles shows (Fig. 5c) similar morphology as that of CM-dextran/ Fe_3O_4 in Fig. 5b,

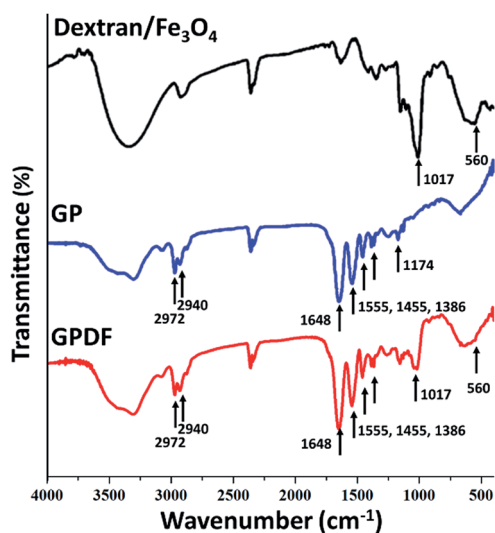


Fig. 3 FT-IR spectra of CM-dextran, GP, and GPDF.

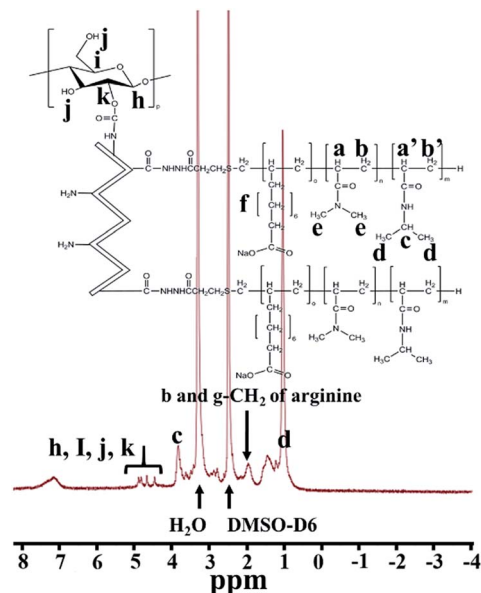


Fig. 4 ^1H -NMR spectra of the GPDF copolymer dissolved in DMSO-D6.

indicating that CM-dextran/ Fe_3O_4 were grafted on the surface of GPDF micelles to provide them with a magnetic property. The GP micelles were slightly larger than the GPDF micelles, which is confirmed by both TEM and DLS, and the results are shown in Table 1.

Fig. 6 shows the thermal decompositions of the dextran/ Fe_3O_4 , GP and GPDF micelles. For dextran/SPIONs and GP, the major polymer decomposition took place at $278\text{ }^\circ\text{C}$ and $354\text{ }^\circ\text{C}$, and 41.3% and 9.1% of the residue was obtained. While for the GPDF polymer, the first major weight loss occurs at $287\text{ }^\circ\text{C}$ and a second weight loss occurs at $383\text{ }^\circ\text{C}$, and 22.7% of the residue was obtained, which indicates that the total amount of iron oxide remaining in sample is 13.6%. The amount of dextran/ Fe_3O_4 linked to GPDF micelle can then be approximated to be 33%.

SQUID magnetometer was used to detect the saturation magnetization of the MNPs and magnetic micelles. As shown in Fig. 7, the saturation magnetizations of CM-dextran/ Fe_3O_4 and GPDF were 22.8 and 7.3 emu g^{-1} , respectively. Both GPDF and CM-dextran/ Fe_3O_4 exhibited superparamagnetism without remanence. The change of magnetization slope can be caused by the dipolar interaction of the neighboring CM-dextran/ Fe_3O_4 assembled on the micelle. The amount of Fe_3O_4 linked to the

Table 1 Measured LCSTs and particle sizes of PNDU, GP, and GPDF at different environmental pHs

Sample	Particle size (nm)	LCST ($^\circ\text{C}$)	
		pH = 6.6	pH = 7.2
PNDU	79.02 ± 0.38	31.4 ± 0.4	32.3 ± 0.6
GP	131.9 ± 4.7	36.3 ± 0.2	38.8 ± 0.2
GPDF	115.8 ± 2.3	37.6 ± 0.4	38.5 ± 0.3



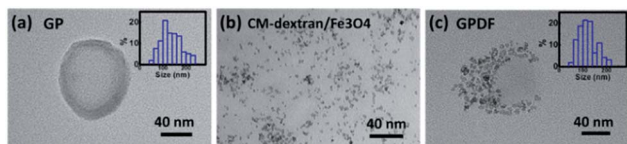


Fig. 5 TEM image of (a) GP micelles, (b) dextran/Fe₃O₄, and (c) GPDF micelles. Insets are the particle's size distribution.

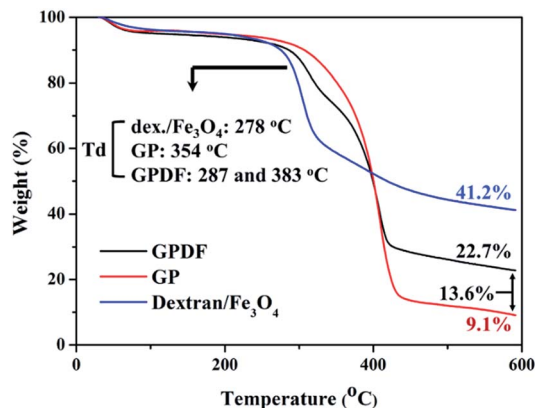


Fig. 6 TGA thermogram of dextran/Fe₃O₄, GP, and GPDF.

GPDF micelle can then be approximated to be 32%, which is consistent with the TGA data.

To simulate the drug release under normal physiological and pathology conditions, hydrophilic molecular nicotine was used in the study. The nicotine has a zeta potential of -10.43 ± 1.62 mV, which can be stably encapsulated in the GPDF micelle during the self-assembly process in an aqueous solution and then remain stable inside the core due to the repulsive forces between the shell layers of GPDF micelles (Fig. S2 of ESI†). On comparing the UV spectra of nicotine-loaded GPDF micelles at both pH 7.5 and pH 6.6, it was

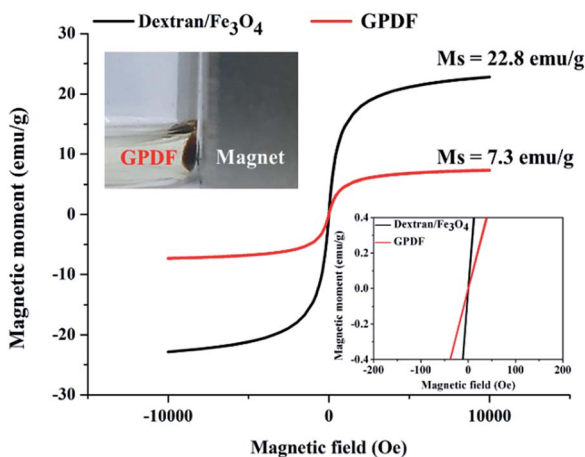


Fig. 7 Magnetic strength of MNP and GPDF as measured by SQUID magnetometer. 22.8 and 7.3 emu g⁻¹ are the saturation magnetization of dextran/Fe₃O₄ and GPDF, respectively.

observed that the micelles at pH 6.6 show a clear nicotine signal at 274 nm (Fig. S3 in ESI†). Fig. 8 shows the release profile of the nicotine-loaded GPDF micelles at pH 7.2 and pH 6.6 at 37.5 °C in 36 h. At pH 7.2, nicotine was released at a very low rate and the amount of release was saturated to about 20% after 36 h. In contrast, under slightly acidic environment (pH 6.6), more than 60% of nicotine was released at enhanced speed.

In previous literature, extracellular acidity is considered as a pathological feature in inflamed regions and tumour areas, where pH values are near 6–7.^{39,40} The present study verified that GPDF micelles could be an efficient way for site-specific and pH-selective drug release. Previously, Wang *et al.* encapsulated magnetic particle inside a micelle to form Fe₃O₄@SiO₂-g-poly-(benzyl-L-aspartate)-g- α -methoxy poly(ethylene glycol) (FeSi@PBLA@mPEG).⁴¹ Rodkate *et al.* fabricated poly(*N*-isopropylacrylamide)/carboxymethylchitosan with magnetic nanoparticles conjugated on the outer layer of the micelle.²⁰ Although the abovementioned reports have shown superparamagnetism in the micelles, the proposed GPDF micelles have higher saturation magnetization with an improved magnetic response, which can be beneficial for the controlled-release drug delivery. In addition, the micelles can carry hydrophilic drugs and their free amine groups and carboxyl group allow them to further conjugate with specific antibodies for target therapy.

Conclusions

In the present study, we synthesized pH-responsive magnetic micelles, gelatin-g-poly(NIPAAm-co-DMAAm-co-UA)-g-dextran/Fe₃O₄. The micelles could specifically identify lesions to normal tissue through environmental pH difference. The micelles may contribute to the accumulation and release of drugs in lesions while reducing the side effects in a normal tissue. In addition, the micelles can carry hydrophilic drugs or undergo further conjugation for target therapy.

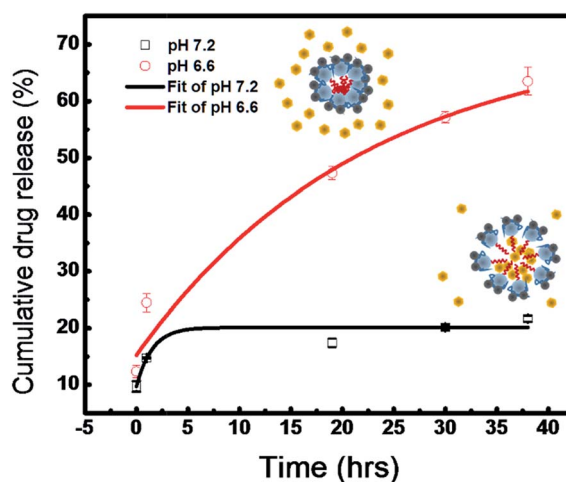


Fig. 8 The accumulative nicotine release from the GPDF micelle at pH 6.6 and 7.2 at 37.5 °C.



Acknowledgements

This work was partly supported by the Ministry of Science and Technology, Taiwan, under Grant no. MOST 104-2112-M-033-008-MY2 and MOST104-2112-M-033-008-MY2, and a grant from Taoyuan General Hospital, Ministry of Health and Welfare.

References

- 1 S. D. Li and L. Huang, *Biochim. Biophys. Acta*, 2009, **1788**, 2259–2266.
- 2 J. Zhao, Y.-D. Chai, J. Zhang, P.-F. Huang, K. Nakashima and Y.-K. Gong, *Acta Biomater.*, 2015, **16**, 94–102.
- 3 Y. Ohya, S. Takeda, Y. Shibata, T. Ouchi, A. Kano, T. Iwata, S. Mochizuki, Y. Taniwaki and A. Maruyama, *J. Controlled Release*, 2011, **155**, 104–110.
- 4 T. Wei, J. Liu, H. Ma, Q. Cheng, Y. Huang, J. Zhao, S. Huo, X. Xue, Z. Liang and X.-J. Liang, *Nano Lett.*, 2013, **13**, 2528–2534.
- 5 J. Liu, Y. Huang, A. Kumar, A. Tan, S. Jin, A. Mozhi and X. J. Liang, *Biotechnol. Adv.*, 2014, **32**, 693–710.
- 6 A. Gothwal, I. Khan and U. Gupta, *Pharm. Res.*, 2016, **33**, 18–39.
- 7 G. H. Gao, Y. Li and D. S. Lee, *J. Controlled Release*, 2013, **169**, 180–184.
- 8 J. Ren, Y. Zhang, J. Zhang, H. Gao, G. Liu, R. Ma, Y. An, D. Kong and L. Shi, *Biomacromolecules*, 2013, **14**, 3434–3443.
- 9 Y. Koyamatsu, T. Hirano, Y. Kakizawa, F. Okano, T. Takarada and M. Maeda, *J. Controlled Release*, 2014, **173**, 89–95.
- 10 P. Mi, H. Cabral, D. Kokuryo, M. Rafi, Y. Terada, I. Aoki, T. Saga, I. Takehiko, N. Nishiyama and K. Kataoka, *Biomaterials*, 2013, **34**, 492–500.
- 11 K. S. Kim, W. Park, J. Hu, Y. H. Bae and K. Na, *Biomaterials*, 2014, **35**, 337–343.
- 12 H. Y. Yang, M. S. Jang, G. H. Gao, J. H. Lee and D. S. Lee, *Nanoscale*, 2016, **8**, 12588–12598.
- 13 J. Cao, S. Huang, Y. Chen, S. Li, X. Li, D. Deng, Z. Qian, L. Tang and Y. Gu, *Biomaterials*, 2013, **34**, 6272–6283.
- 14 Z. Ye, J. Guo, D. Wu, M. Tan, X. Xiong, Y. Yin and G. He, *Carbohydr. Polym.*, 2015, **132**, 520–528.
- 15 L. Wu, C. Ni, L. Zhang and G. Shi, *J. Biomater. Sci., Polym. Ed.*, 2016, **27**, 643–656.
- 16 H. Li, H. Jiang, M. Zhao, Y. Fu and X. Sun, *Polym. Chem.*, 2015, **6**, 1952–1960.
- 17 N. Ma, Y. Li, H. Xu, Z. Wang and X. Zhang, *J. Am. Chem. Soc.*, 2010, **132**, 442–443.
- 18 M. L. Kang, J. E. Kim and G. I. Im, *Acta Biomater.*, 2016, **39**, 65–78.
- 19 H. I. Seo, A. N. Cho, J. Jang, D. W. Kim, S. W. Cho and B. G. Chung, *Nanomedicine*, 2015, **11**, 1861–1869.
- 20 N. Rodkate and M. Rutnakornpituk, *Carbohydr. Polym.*, 2016, **151**, 251–259.
- 21 M. Bikram and J. L. West, *Expert Opin. Drug Delivery*, 2008, **5**, 1077–1091.
- 22 D. Roy, W. L. A. Brooks and B. S. Sumerlin, *Chem. Soc. Rev.*, 2013, **42**, 7214–7243.
- 23 J. Liu, A. Debuigne, C. Detrembleur and C. Jérôme, *Adv. Healthcare Mater.*, 2014, **3**, 1941–1968.
- 24 K. Lava, B. Verbraeken and R. Hoogenboom, *Eur. Polym. J.*, 2015, **65**, 98–111.
- 25 P. Yu, H. Yu, C. Guo, Z. Cui, X. Chen, Q. Yin, P. Zhang, X. Yang, H. Cui and Y. Li, *Acta Biomater.*, 2015, **14**, 115–124.
- 26 *Multifunctional Pharmaceutical Nanocarriers*, ed. V. P. Torchilin, Springer, New York, 2008.
- 27 Y. Masayuki, M. Mizue, Y. Noriko, O. Teruo, S. Yasuhisa, K. Kazunori and I. Shohei, *J. Controlled Release*, 1990, **11**, 269–278.
- 28 J.-C. Yeh, H.-H. Yang, Y.-T. Hsu, C.-M. Su, T.-H. Lee and S.-L. Lou, *Colloids Surf., A*, 2013, **421**, 1–8.
- 29 S. Young, M. Wong, Y. Tabata and A. G. Mikos, *J. Controlled Release*, 2005, **109**, 256–274.
- 30 W.-M. Li, D.-M. Liu and S.-Y. Chen, *J. Mater. Chem.*, 2011, **21**, 12381–12388.
- 31 A. K. Gupta, M. Gupta, S. J. Yarwood and A. S. Curtis, *J. Controlled Release*, 2004, **95**, 197–207.
- 32 T. Kean and M. Thanou, *Adv. Drug Delivery Rev.*, 2010, **62**, 3–11.
- 33 R. Riva, H. Ragelle, A. des Rieux, N. Duhem, C. Jérôme and V. Pr eat, in *Chitosan for Biomaterials II*, ed. R. Jayakumar, M. Prabakaran and R. A. A. Muzzarelli, Springer Berlin Heidelberg, Berlin, Heidelberg, 2011, pp. 19–44, DOI: 10.1007/12_2011_137.
- 34 M. S. Lee, C. M. Su, J. C. Yeh, P. R. Wu, T. Y. Tsai and S. L. Lou, *Int. J. Nanomed.*, 2016, **11**, 4583–4594.
- 35 H. Nemala, J. Thakur, V. Naik, P. Vaishnav, G. Lawes and R. Naik, *J. Appl. Phys.*, 2014, **116**, 034309.
- 36 K.-W. Huang, *Int. J. Nanomed.*, 2012, **7**, 2987–2996.
- 37 S. Patra, E. Roy, P. Karfa, S. Kumar, R. Madhuri and P. K. Sharma, *ACS Appl. Mater. Interfaces*, 2015, **7**, 9235–9246.
- 38 D. Chen, N. Li, X. Xia, Q. Xu, J. Ge, Y. Li, J. Lu and H. Gu, *J. Controlled Release*, 2011, **152**(1), e67–e68.
- 39 L. Dong, Z. Li, N. R. Leffler, A. S. Asch, J. T. Chi and L. V. Yang, *PLoS One*, 2013, **8**, e61991.
- 40 P. Vaupel, F. Kallinowski and P. Okunieff, *Cancer Res.*, 1989, **49**, 6449–6465.
- 41 J. Wang, C. Gong, Y. Wang and G. Wu, *RSC Adv.*, 2014, **4**, 15856–15862.

